International Journal of Engineering and Science Applications
ISSN 2406-9833

IJEScA

IDENTIFICATION OF PALU-KORO FAULT MECHANISM AND EARTHQUAKE HAZARD VULNERABILITY OF PALU AREA CENTRAL OF SULAWESI

J. Nugraha[1,2], A. Jaya[1], I. Alimuddin[1]
[1]*Department of Geology, Hasanuddin University, Makassar, 90245, Indonesia*
[2]*Indonesia Agency for Meteorology, Climatology & Geophysics, Jakarta, 10720, Indonesia*
e-mail : jimmi.nugraha@gmail.com

ABSTRACT

The identification of the Palu-Koro Fault and earthquake hazard vulnerability study has been conducted based on multi-criteria analysis which is a recent innovation zonation method of earthquake hazard vulnerable areas. The study method used is a merging scientific discipline of geology and geophysics. Field data collection (acquisition), processing, data analysis and modeling in the laboratory using several seismic software became the main framework in this study. Earthquake hazard vulnerability maps contain several criteria related to factors affecting the vulnerability level in the study area to the earthquakes hazard. Acquisition of geological investigation including fault-slip at 19 points and historical of 30 earthquakes data were used to verified fault type or earthquake focal mechanism. Microtremor measurements were conducted at 350 points throughout at the Palu area to analyze the vulnerability of earthquake hazard in the study area. The earthquake focal mechanism analysis shows the type of fault that predominantly controls through the Palu area and its surroundings controlled by strike-slip or horizontal fault mechanism. The micro-zonation analysis shows that the value of the resonant frequency (fo) in the range of 0.307 to 14.668, amplification factor (A) in the range of 1.297 to 8.946, the predominant period (Tg) in the range of 0.068 to 3.257, seismic vulnerability (Kg) in the range of 0.36 to 231, 97. Based on the vulnerability classification level and earthquake hazard shows that no area is safe. Particularly the impact caused by an earthquake due to the activity of Palu-Koro Fault.

Keywords: Palu-Koro Fault; resonant frequency; fault mechanism; soil vulnerability; earthquake.

1. INTRODUCTION

Palu-Koro Fault in central of Sulawesi viewed from the satellite image is a series of valley that seen as far as 200 km south of Palu Bay (1). No estimation slip rate that has ever been derived refers to stream offsets from this fault [2] [1]. Physiography of the Palu area is consists of east to west ridge [3]. The geomorphologic condition of the study area is controlled by height difference and geology processes.

Palu area includes structural morphology consist of mountains, hills, and plain area (Palu Valley), topographical condition as shown in Figure 1. Refers to BMKG data since 2009 in the Palu-Koro Fault and surrounding areas, an average of more than 3,000 earthquakes occurs in a year, both felt or not [4]. Katili [2] reports that earthquakes in 1905, 1907, and 1934 occurred near Palu-Koro Fault trace already known, however the magnitude and its accuracy location not available.

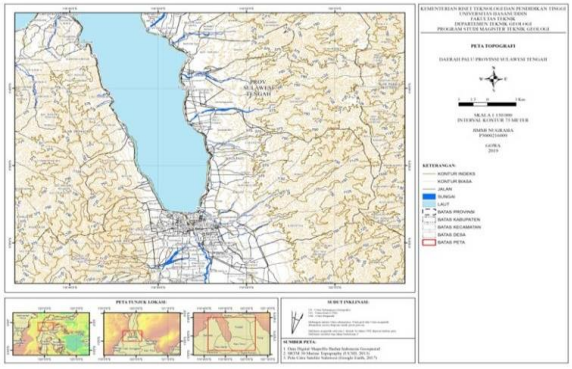

Fig. 1. Topography map of the study area.

Earthquake ruin others reported also occur in Sesar Palu-Koro in 1909 [1]. Study of micro-seismicity conducted for two weeks in 1978 records a few seismicities from this fault [5] and some record earthquake epicenter globally (1964-1995) on fault trace [6]. Havard Centroid Moment Tensor (CMT) catalog only have content of two earthquake (Mw 5.9 and Mw 6.0 on October 1998) occurred to its fault.

Palu-Koro Fault has a strike-slip movement lateral-left between Molluca coastal plate [7] and the Sunda plate [8]. GPS provides an assessment that current fault locked, slip that occurred is not aseismic. A Slip rate of approximately 40mm/year occurs in Palu-Koro. Bellier [9] report paleoseismology fact for three events of slip surface on the Palu-Koro Fault segment in 2000.

The focal mechanism parameter of the earthquake provides critical information for vulnerability analysis earthquake and local study tectonic, regional, and global [10]. The focal mechanism of earthquakes is geometric representation shifting fractures at the time when the earthquake happens [11]. Focal mechanism solution generally used for the study of characteristic tectonic in a region and required as input to resolve estimation stress tectonic problem (Figure 2).

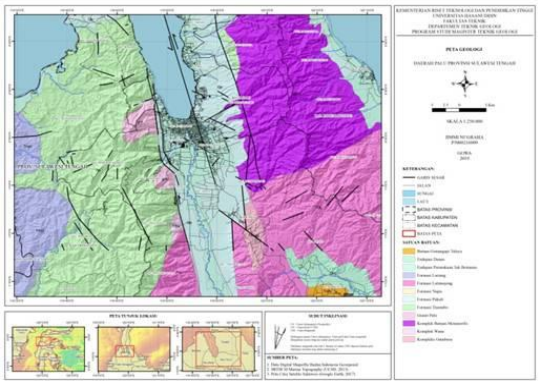

Fig. 2. Geology map of the study area.

Microtremor or also known as ambient noise is ground vibration which is caused by some factors like traffic, industry, and other human activities on the earth. Besides human activities, microtremor sources also caused by natural factors, like air interaction and building structure, sea current and sea wave long period [12].

Microtremor survey observation was obtained to find characteristics of dynamic subsoil surface, such as resonance frequent and vulnerability seismic index [13]. Analysis of microtremor data using Horizontal to Vertical Spectrum Ratio (HVSR) method [14].

The level of damage in a place depends not only on the magnitude of the earthquake and its distance from the epicenter but also on local geological conditions that highly affect [15]. The phenomenon is known as the local site effect due to an earthquake. The local site effect occurs caused contrast impedance with the presence of a layer of fine sedimentary material on the bedrock [16]. At the time when an earthquake occurs, the surface sedimentary layer multi-reflection seismic waves between the bedrock and surface sediment layer shown in Figure 3 [17].

Examined the relationship between seismic vulnerability index and damage ratio has been studied using the 1995 Kobe earthquake data.

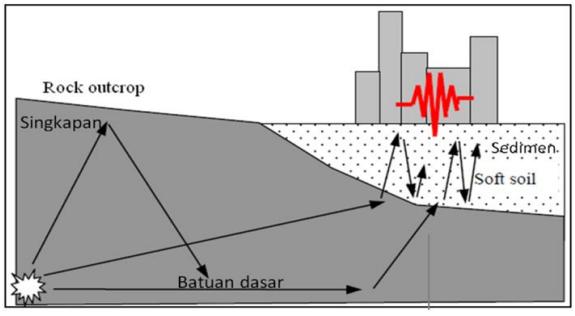

Fig. 3. Seismic waves are trapped in the sedimentary layer [17].

The results of the study showed that the distribution of high seismic vulnerability indexes was located in the severely damaged zones spread by forming damage pathways. The distribution of the high seismic vulnerability index is located along the coast. The phenomenon of liquefaction is often found in the region [14].

2. METHODOLOGY

The purpose of this study is to do the mechanism study of Palu-Koro Fault and its implications to the vulnerability of earthquake hazard in Palu Central of Sulawesi.

The purpose of this research:

A. Identify the mechanism of Palu-Koro Fault refers to geology and geophysics data.

B. The apping vulnerability of earthquake hazard in Palu Central of Sulawesi refers to the predominant period and amplification factor in the vulnerability level of the earthquake hazard map.

Earthquake hazard vulnerability map in Palu Central of Sulawesi refers to multicriteria analysis is a map model of vulnerability level of earthquake hazard is the latest innovation in zonation method earthquake vulnerable area. Map results can be utilized as a reference for community and related parties in an attempt to disaster mitigation earthquake and regional arrangement safely toward development planning.

This study using two approaches, geological and geophysical method. Map results can be utilized as a reference for community and related parties in an attempt to disaster mitigation earthquake and arrangement safely toward development planning. This study using two approaches, geological and geophysical method.

A. Geological Method

A.1 Determination of data collection points (plotting), by using the Global Positioning System (GPS).

A.2. Outcrop observation, covering description and outcrop photo.

A.3. Lithology description.

A.4. Sampling rock outcrops by spot sampling method hand specimen sized.

A.5. Identification distribution lithology refers to aged and level of destruction.

A.6 Acquisition of structure data for 19 points including joint, direction of foliation, fault-slip in the form of slickenside or fracture plane and slicken line consisting of striation and plunge orientation (Figure 4).

B. Geophysical Research

B.1 Fault mechanism data was obtained through seismic wave data of earthquake events recorded in seismometer in the study area through the catalog of IRIS (Incorporated Institute for Seismology) at http://ds.iris.edu [18].

B.2 Microtremor data collection refers to standard procedure predefined by SESAME European Research Project. The study was carried out by survey and collecting field data using seismometer portable in Palu and the surroundings.

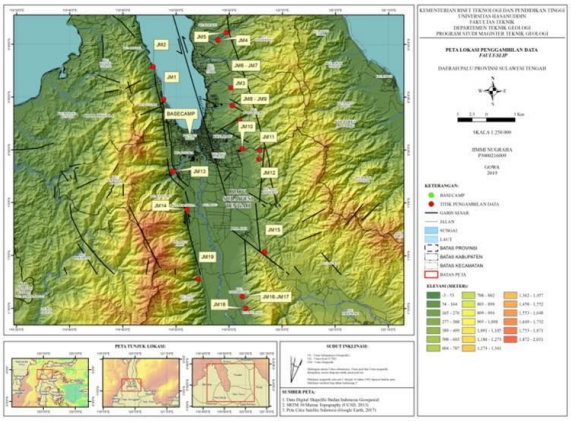

Fig. 4. Map of location for acquisition fault-slip data.

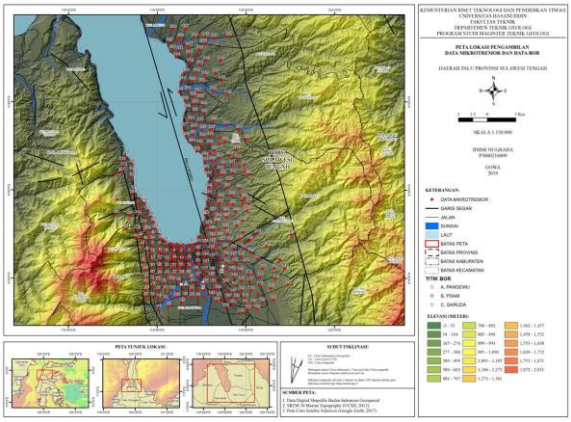

Fig. 5. Map of location for acquisition microtremor.

Data collection was carried out as many as 350 points with a distance between points of about 500 meters (Figure 5). The duration of data collection for every point is about 30 minutes.

3. Result And Discussion

The study field data geology structure is in the form fault-slip consist of measurement slickenside data (strike and dip) and slickenline (striation and plunge) furthermore processed using MIM (Multiple Inverse Method) 2010 software. Result of fault data analysis (slickenside and slickenline) in the study area in Figure 6 and Appendix 1 a and b.

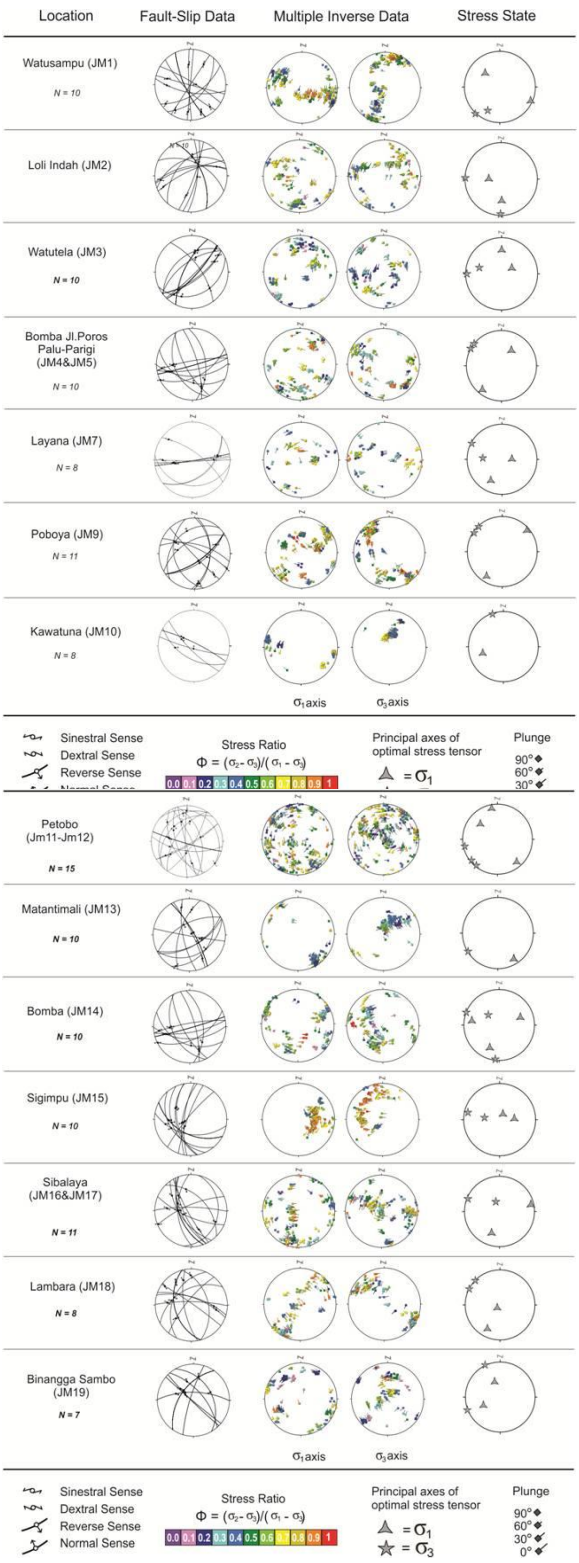

Fig. 6. The results of processing the fault-slip data are processed using the Multiple Inverse Method (MIM) [19].

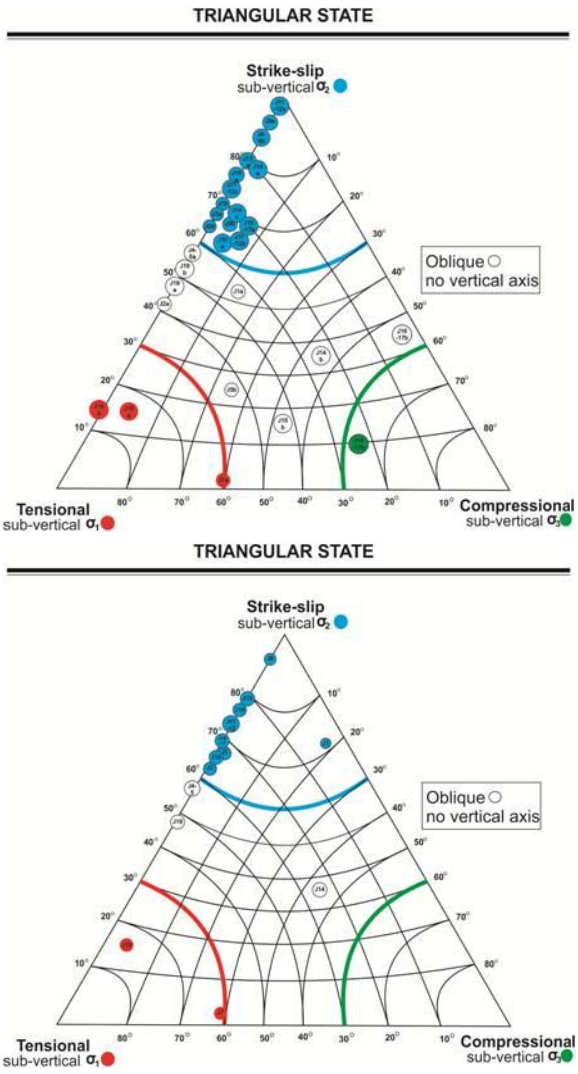

Fig. 7. Earthquake focal mechanism data in the triangle diagram [20].

Based on the value of affirmation, the type of fault according to Anderson's classification (1951) at the study location in sequence as follows:

- Watusampu area, West Palu (JM1) are oblique and strike-slip fault.
- The Loliindah area, Donggala (JM2) are oblique and strike-slip fault.
- Watutela area (JM3) are strike-slip and oblique fault.
- Bomba area, Parigi Palu Street (JM4-JM5) are oblique and strike-slip fault.
- Layana area (JM7) are normal and strike-slip fault.
- Poboya area (JM9) is a strike-slip fault.
- Kawatuna area (JM10) is a strike-slip fault.
- Petobo area (JM11-JM12) is a strike-slip fault.
- Matantimali area (JM13) is a strike-slip fault.
- Bomba, Sigi area (JM14) are strike-slip, oblique, and strike-slip faults.
- Sigimpu area (JM15) are normal and strike-slip fault.
- Sibalaya area (JM16-JM17) are strike-slip and oblique fault.
- Lambara area (JM18) are strike-slip and normal fault.
- Binangga Sambo area (JM19) is an oblique fault.

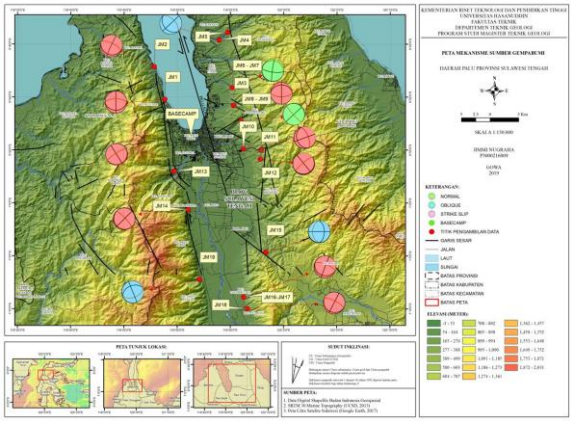

Fig. 8. Plotting result of fault data analysis (slickenside and slickenline), population data of earthquake focal mechanism based on the field survey in the research area.

Plotting result stress state data on the Frochlich triangle diagram shows that fault population (geology structure) which control study area are oblique, strike-slip and normal fault. The dominant fault is a horizontal fault or strike-slip fault (Figure 8). Search of IRIS catalog was obtained 30 focal mechanism data result analysis earthquake in 1985-2018 on coordinate 0º15’00” NL – 1º27’00” SL and 119º18’00” - 120º27’00” EL (Appendix 2). Analysis and plotting data were done using the software instrument system monitoring earthquake JISView 1.1 version, Linuh 1.0.2/Ultimate result development of Puslitbang BMKG (Figure 9).

Data population of earthquake focal mechanism shows that fault type control study areas are strike-slip, oblique-normal, normal and thrust. The dominant fault is horizontal fault or strike-slip fault, that 16 data or 53.3% from the population with depth hypocenter less than 70 km (shallow earthquake) as shown in Figure 10.

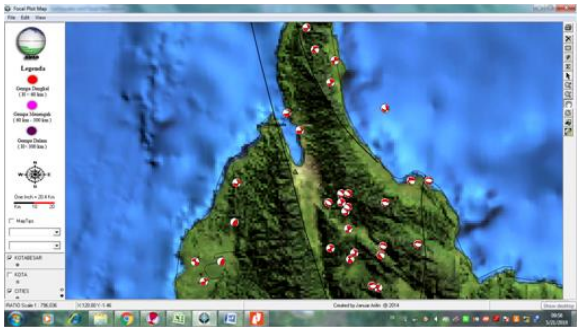

Fig. 9. Map of earthquake focal mechanism based on a catalog of earthquake events in the research area [21].

Fig. 10. Statistical clustering of population data of earthquake focal mechanism based on the catalog of earthquake events (historical data) in the research area. [21].

Referring to historical data of significant earthquakes, the pattern of earthquake mechanisms and parameters occurring in the Palu area and its surroundings indicates that the Palu-Koro Fault remains active until now. Microtremor measurement on 350 points since May 21, 1985, to August 25, 2018, was obtained data and result processing also the analysis as follow:

A. Value of resonance frequency (fo) in range 0.307 to 14.686 (Figure 11), where dominant value is fo lower than 2.5 found in 319 points. The highest fo value in 4 points with value 11.174 to 14. 686.

B. Value of amplification factor (A) in range 1.297 to 8. 946 (Figure 12), where dominant value A lower than 3.0 found in 230 points. A value that very high found in 4 points with 6.622 to 8.964.

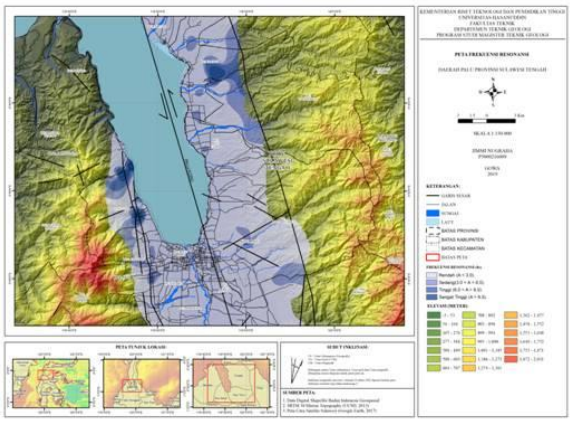

Fig. 11. Map of the resonance frequency map of the study area.

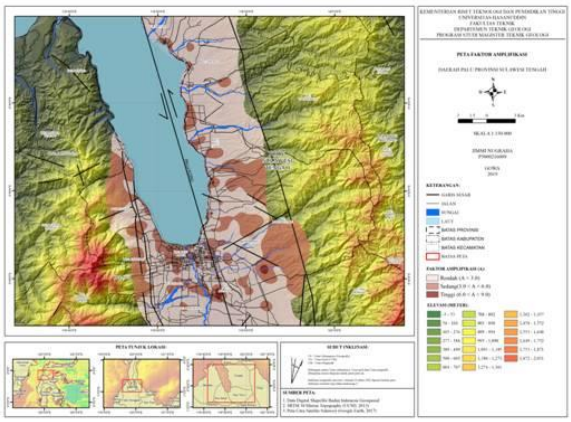

Fig. 12. Map of the resonance frequency map of the study area.

C. Value of the predominant period (Tg) in range 0.08 to 3.257 (Figure 13), where the dominant value is Tg higher than 0.4 found in 319 points. Tg value higher than 0.4 indicates soft soil.

D. Value of Vulnerability seismic (Kg) in the range 0. 36 to 231.97 (Figure 14), where the dominant value is Kg lower than 10.0 found in 187 points. Kg value that very

high with 30.050 to 231.97 found in 19 points station.

Referring to the vulnerability level classification of its earthquake hazard seen that no area is safe. Some factors influence vulnerability index seismic; they are generally sediment deposits that compile the research area consist of alluvial and Molasa deposits.

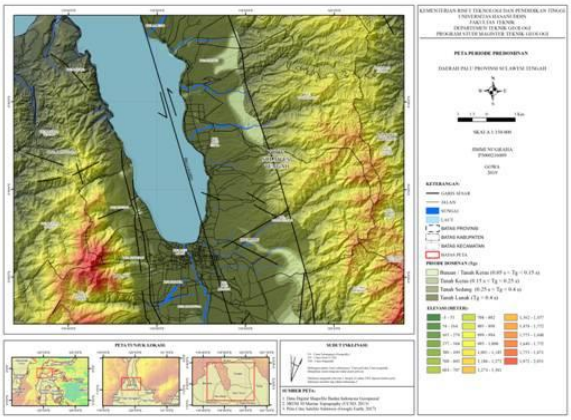

Fig. 13. Map of the predominant period of the study area.

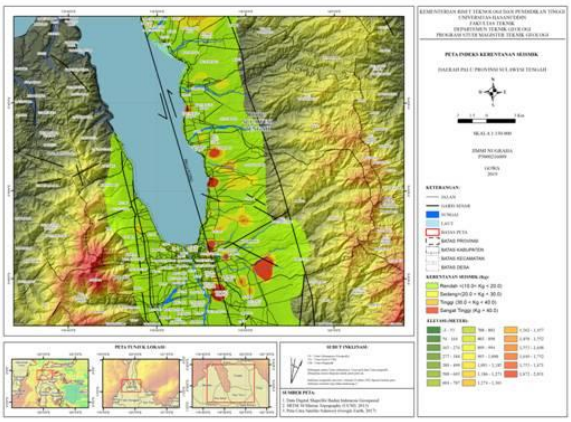

Fig. 14. Map of the seismic vulnerability index of the study area.

Alluvial deposits inshore area to urban area while in foothills area sediment deposits Molasa Quarterly aged has low solidity level. Loose material (unconsolidated) is a factor that influences high-level vulnerability seismic due to affect amplification factor scale when an earthquake happens.

Moreover the depth of groundwater including significant factors in vulnerability seismic, when an earthquake in shallow groundwater zone, liquefaction can be happening. For some station points in Balaroa, that level vulnerability is high, indicated the average groundwater level less than 2 meters.

The lithology area compiler particularly is alluvial sediment, Molasa sediment that contains sandstone and conglomerate also sediment stone Tinombo Formation that contains shale, sandstone, and conglomerate. In areas with low to very high vulnerability values compiled by lithology alluvial deposits and Molasa sediment consisting of sandstone, and conglomerate, where these rocks are not well consolidated.

There is a similarity in the pattern between the seismic vulnerability index and the damage ratio. Location with high vulnerability index values has experienced severe damage as indicated by a high damage ratio. Otherwise locations with a low seismic vulnerability index, then the location experienced minimal damage that is reflected in the low damage ratio.

The relationship between the seismic vulnerability index based on microtremor with damage ratio shows a positive correlation at each microtremor measurement location. The results of the study are not fully correlated with the damage caused by the earthquake on September 28, 2018. The main factor of the damage that occurred at that time was dominantly caused by tsunami disaster (Figure 15).

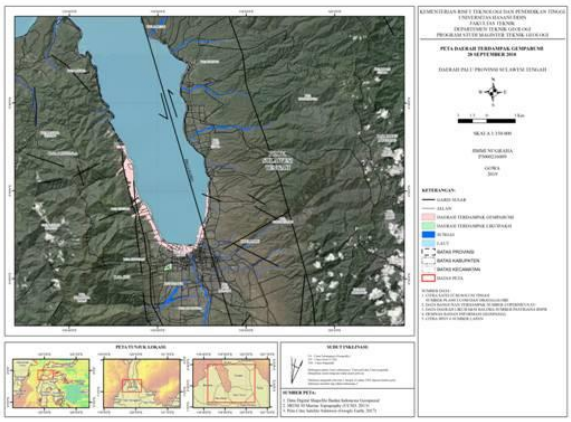

Fig. 15. Map of the earthquake-affected area September 28, 2018, of the study area.

4. CONCLUSIONS

Data collection results, processing, analyzing and discussion also verification, this study can be concluded as follow:

A. Plotting stress state data on the Frochlich triangle diagram and data history earthquake shows that fault population (geology structure) control study area are oblique, strike-slip and normal fault. The dominant fault is horizontal fault or strike-slip fault.

B. This refers to the vulnerability level classification of the earthquake hazard seen that no area is safe. Particularly the impact caused by an earthquake due to the activity of Palu-Koro Fault.

This study was conducted as a hypothesis test result or achievement of the research objective. Hopefully, this study could be implemented particularly in science development and as a reference development area based on risk reduction of earthquake by utilizing earthquake hazard vulnerability maps based on multi-criteria analysis.

ACKNOWLEDGMENT

Thank you for the students of the Department of Geological Engineering for all their support and assistance, especially to Sandy Tias Setiawan, Bagus Firmansyah and Citra Aryani Anwar. Special thank you for the Palu Geophysics Station of BMKG, Cahyo Nugroho, S.Si as Station Head, Sofian, S.Si as Head of Data and Information Section and staff who have assisted in data collection and various parties for their support in this study.

REFERENCES

[1] Hamilton, W., 1979, Tectonic of Indonesia Region, United States Geological Survey Professional Paper, United States Government Printing Office, Washington, 1078, 345 pp.

[2] Katili, J.A., 1970, Large Transcurrent Faults in Southeast Asia with Special Reference to Indonesia, Geol. Rundshc., 59, 581-600.

[3] Sukamto, R., 1973, Peta Geologi Tinjau Lembar Palu, Sulawesi–Skala 1:250.000, Departemen Pertambangan dan Energi, Pusat Penelitian dan Pengembangan Geologi, Bandung.

[4] BMKG, 2018, *Data Gempa Bumi di Indonesia*, melalui http://inatews.bmkg.go.id/new/query_gmp_dirasakan.php, diakses pada 10 Oktober 2018 pukul 15.00

[5] McCaffrey, R. & Sutardjo, 1982, Reconnaissance Microearthquake Survey of Sulawesi, Indonesia, Geophysics Research Letters, Vol. 9, No. 8, p. 793-796, August.

[6] Engdahl, E.R., Van der Hilst, R.D., & Bulard, R.P., 1998, Global Teleseismic Earthquake Relocation With Improved Travel Times and Procedures for Depth

Determination, Bull. Seism. Soc. Amer., 88, 722-743.

[7] Bird, P., 2003, An Updated Digital Model of Plate Boundaries: Geochemistry, Geophysics, Geosystems, 4, no. 3, 1027, doi:10.1029/2001GC000252.

[8] Stevens, C., 1999, GPS Measurements of Crustal Deformation in Eastern Indonesia and Papua New Guinea, Ph.D. Thesis, Ransselaer Polytechnic Institute, Troy, New York.

[9] Bellier, O., Sebrier, M., Beaudouin, dkk., 2001, High Slip Rate for A Low Seismicity Along the Palu-Koro Active Fault in Central Sulawesi (Indonesia), Terra Nova, v. 13, p. 463-470.

[10] Oros, E., Popa, M., Popescu, E., & Moldovan, I.A., 2007, Seismological Database for Banat Seismic Region (Romania)–Part 2: The Catalogue of the Focal Mechanism Solutions, Rom. Journ. Phys, 53, 7-8, P. 965–977.

[11] Walsh, D., 2008, Directional Statistics, Bayesian Methods of Earthquake Focal Mechanism Estimation, and Their Application to New Zealand Seismicity Data, New Zealand: Thesis, Victoria University of Wellington.

[12] Motamed, R., Ghalandarzadeh, A., Tawhata, I., & Tabatabei, S.H., 2007, Seismic Microzonation and Damage Assessment of Bam City, Southern Iran, Journal of Earthquake Engineering, 11:110-132.

[13] Nakamura, Y., 2000, Clear Identification of Fundamental Idea of Nakamura's Technique and Its Application, In: Proceedings of 12th World Conference on Earthquake Engineering, New Zealand.

[14] Nakamura, Y., 1989, A Method for Dynamic Characteristic Estimatimation of Subsurface Using Microtremor on The Ground Surface, Japan: Quarterly Report of Railway Technical Research Institute (RTRI), Vol.30, No.1, p. 25-33.

[15] Naeni, S.A., & Zarincheh, A., 2010, Site Effects and Seismic Hazard Analysis of Kermanshah Region of Iran, Journal of Applied Science 10 (19): 2231-2240.

[16] Zaharia, B., Radulian, M., Popa, M., Grecu, B., Bala, A. & Tataru, D., 2008, Estimation of the Local Response Using the Nakamura Method for the Bucharest Area, Romanian Report in Physics, Vol. 60, No. 1, P. 131-144.

[17] Tuladhar, R., 2002, Seismic Microzonation of Greather Bangkok Using Microtremor, Thesis, Asian Institute of Technology, School of Civil Engineering, Thailand.

[18] Yamaji, A., 2000, *The Multiple Inverse Method: A New Technique to Separate Stresses from Heterogeneous Fault-Slip Data*, Journal of Structural Geology 22, 441-452.

[19] Frohlich, C., 1992, *Triangle Diagrams: Ternary Graphs to Display Similarity and Diversity of Earthquake Focal Mechanisms*. Physics of the Earth and Planetary Interiors, 75(1-3), 193-198.

[20] Nugraha, J., & Arifin, J., 2014, *JISView: Penentuan Mekanisme Sumber Gempa Bumi Berbasis Sistem Informasi Geografi*, Buletin Artikel Ilmiah MKKUG 2014 Balai II BMKG Vol. 4 No. 8 Agustus 2014, 44–60, ISSN: 2088-9151.

[21] IRIS, 2018, *IRIS Earthquake Browser (IEB)*, melalui https://www.iris.edu/ieb/, diakses pada 15 Oktober 2018 pukul 10.00

Appendix 1a. Results of fault-slip data processing in the study area using MIM 2010 software.

No.	Location	Coordinate		Lithology and units lithology	Number of fault datasets	Stress states	σ_1	σ_3	Φ	Number of datasets compatible with the tensor	Fault Type
		Latitude (°)	Longitude (°)								
1	WATUSAMPU, PALU BARAT (JM1)	-0.838	119.814	Porfiri Basalt (Volcanic Rock)	10	A	312/33	46/14	0.4	4	Oblique
						B	115/4	206/19	0.2	5	Strike Slip
2	LOLIINDAH DONGGALA (JM2)	-0.786	119.797	Porfiri Basalt (Volcanic Rock)	10	A	272/49	182/0	0.2	3	Oblique
						B	180/26	270/0	0.1	3	Strike Slip
3	WATUTELA (JM3)	-0.846	119.922	Granite (Intrusive Rock)	10	A	360/24	270/0	0.2	5	Strike Slip
						B	59/55	286/25	0.3	4	Oblique
4	BOMBA (JALAN POROS PALU PARIGI) (JM4-JM5)	-0.742	119.901	Arkosic Arenit (Sandstone)	5	A	30/33	300/0	0.6	7	Oblique
						B	217/8	307/0	0.2	3	Strike Slip
5	LAYANA (JM7)	-0.819	119.919	Granodiorite (Intrusive Rock)	8	A	88/60	271/30	0.3	4	Normal
						B	207/22	297/0	0.2	3	Strike Slip
6	POBOYA (JM9)	-0.871	119.933	Porfiri Granodiorite (Intrusive Rock)	11	A	47/5	317/0	0.4	7	Strike Slip
						B	214/13	304/0	0.7	5	Strike Slip
7	KAWATUNA (JM10)	-0.914	119.937	Quartz Wacke (Sandstone)	8	A	250/26	340/0	0.1	4	Strike Slip
8	PETOBO (JM11-JM12)	-0.918	119.961	Gneiss Jadeit Albite Quatrz (Metamorphic Complex)	15	A	348/2	258/0	0.2	6	Strike Slip
						B	309/23	192/06	0	5	Strike Slip
						C	141/8	231/0	0.1	5	Strike Slip
9	MATANTIMALI (JM13)	-0.951	119.829	Granodiorite (Intrusive Rock)	10	A	148/10	238/0	0.2	7	Strike Slip
10	BOMBA, SIGI (JM14)	-1.010	119.850	Schist Silimanite Quartz (Schist)	10	A	277/10	187/0	0.1	4	Strike Slip
						B	70/26	310/44	0.3	6	Oblique
						C	201/20	291/0	0.4	5	Strike Slip
11	SIGIMPU (JM15)	-1.078	119.97	Gneiss Biotite Quartz (Gneiss)	10	A	30/72	281/6	0.4	5	Normal
						B	84/46	275/43	0.8	7	Oblique
12	SIBALAYA (JM16-JM17)	-1.148	119.937	Quartz Arenite (Meta Sandstone)	11	A	201/21	291/0	0.1	5	Strike Slip
						B	79/6	338/58	0.4	4	Oblique
13	LAMBARA (JM18)	-1.166	119.942	Arkose Wacke (Meta Sandstone)	10	A	207/16	297/0	0.1	5	Strike Slip
						B	223/77	313/0	0.6	4	Normal
14	BINANGGA SAMBO (JM19)	-1.121	119.868	Diorite (Intrusive Rock)	7	A	338/42	248/0	0.1	3	Oblique
						B	244/34	334/0	0.2	3	Oblique

Appendix 1b. Results of fault-slip data processing in the study area using MIM 2010 software.

No.	Location	Coordinate		Lithology and units lithology	Number of fault datasets	σ_1	σ_3	Φ	Number of datasets compatible with the tensor	Fault type
		Latitude (°)	Longitude (°)							
1	WATUSAMPU, PALU BARAT (JM1)	-0.838	119.814	Porfiri Basalt (Volcanic Rock)	10	115/4	206/19	0.2	5	Strike Slip
2	LOLIINDAH DONGGALA (JM2)	-0.786	119.797	Porfiri Basalt (Volcanic Rock)	10	180/26	270/0	0.1	3	Strike Slip
3	WATUTELA (JM3)	-0.846	119.922	Granite (Intrusive Rock)	10	360/24	270/0	0.2	5	Strike Slip
4	BOMBA (JALAN POROS PALU-PARIGI) (JM4)	-0.742	119.901	Arkosic Arenit (Sandstone)	5	227/33	317/0	0.3	7	Oblique
5	LAYANA (JM7)	-0.819	119.919	Granodiorite (Intrusive Rock)	8	205/74	98/5	0.1	1	Normal
6	POBOYA (JM9)	-0.871	119.933	Porfiri Granodiorite (Intrusive Rock)	11	47/5	317/0	0.4	7	Strike Slip
7	KAWATUNA (JM10)	-0.914	119.937	Quartz Wacke (Sandstone)	8	250/26	340/0	0.1	4	Strike Slip
8	PETOBO (JM11-JM12)	-0.918	119.961	Gneiss Jadeit Albite Quatrz (Metamorphic Complex)	15	141/8	231/0	0.1	5	Strike Slip
9	MATANTIMALI (JM13)	-0.951	119.829	Granodiorite (Intrusive Rock)	10	148/10	238/0	0.2	7	Strike Slip
10	BOMBA, SIGI (JM14)	-1.010	119.850	Schist Silimanite Quartz (Schist)	10	226/9	316/0	0.4	4	Strike Slip
11	SIGIMPU (JM15)	-1.078	119.97	Gneiss Biotite Quartz (Gneiss)	10	91/51	269/38	0.4	14	Oblique
12	SIBALAYA (JM16-JM17)	-1.148	119.937	Quartz Arenite (Meta Sandstone)	11	201/21	291/0	0.1	5	Strike Slip
13	LAMBARA (JM18)	-1.166	119.942	Arkose Wacke (Meta Sandstone)	10	207/16	297/0	0.1	5	Strike Slip
14	BINANGGA SAMBO (JM19)	-1.121	119.868	Diorite (Intrusive Rock)	7	338/42	248/0	0.1	3	Oblique

Appendix 2. Data catalog of earthquake events in the 1985-2018 (IRIS).

No.	Earthquake Event			Time (UTC)			Coordinate		Magnitude		Depth (km)	Nodal Plane 1			Nodal Plane 2			T (σ1)		N (σ2)		P (σ3)		Fault Type
	Day	Month	Year	Hour	Minute	Second	Latitude (º)	Longitude (º)	Strength	Type		Strike (º)	Dip (º)	Rake (º)	Strike (º)	Dip (º)	Rake (º)	Azimuth (º)	Plunge (º)	Azimuth (º)	Plunge (º)	Azimuth (º)	Plunge (º)	
1	30	9	2018	14	38	43	-1.25	120.24	5.1	MW	26.1	111	35	-86	286	55	-93	18	10	288	2	185	80	Normal
2	29	9	2018	10	30	17	-1.43	120.19	5.1	MW	12	116	37	-56	256	60	-112	2	13	268	19	123	67	Oblique-Normal
3	28	9	2018	21	24	1	-1.44	120.22	5	MW	12	127	59	4	35	87	149	346	24	210	58	85	19	Strike-slip
4	**28**	**9**	**2018**	**10**	**2**	**59**	**-0.72**	**119.86**	**7.6**	**MW**	**12**	**348**	**57**	**-15**	**87**	**77**	**-146**	**214**	**13**	**105**	**54**	**312**	**33**	Strike-slip
5	28	9	2018	8	24	57	-0.4	120.02	5.2	MW	12	181	77	-1	272	89	-167	46	8	274	77	137	9	Strike-slip
6	28	9	2018	7	0	2	-0.25	119.89	6.1	MW	12	359	66	-14	95	77	-155	225	8	120	62	319	27	Strike-slip
7	2	11	2017	17	2	15	-1.29	120.23	4.9	MW	14.8	268	30	-143	145	72	-65	216	23	317	24	87	56	Oblique-Normal
8	29	5	2017	14	35	28	-1.24	120.40	6.6	MW	12	111	34	-78	277	57	-98	13	12	282	6	163	77	Normal
9	7	9	2016	14	32	40	-0.95	120.37	5.3	MW	12	159	38	-22	267	76	-126	24	23	277	35	140	46	Oblique-Normal
10	23	2	2014	15	6	53	-1.05	120.25	5.4	MW	12.9	114	28	-79	282	63	-96	16	18	285	5	180	71	Normal
11	30	6	2013	1	4	20	-0.64	119.80	4.9	MW	28.2	330	38	-19	75	79	-126	192	25	83	36	309	44	Oblique-Normal
12	18	8	2012	9	41	56	-1.26	120.00	6.3	MW	12.5	339	83	-5	70	85	-173	205	1	106	81	295	9	Strike-slip
13	8	2	2012	8	52	23	-0.35	119.93	4.8	MW	12.7	250	62	-161	151	73	-30	203	8	304	56	108	33	Strike-slip
14	19	12	2011	1	23	26	-1.14	119.56	5.6	MW	12.3	17	21	72	216	70	97	136	64	34	6	301	25	Thrust
15	8	1	2011	8	15	13	-1.05	120.05	5	MW	23.3	73	74	-178	343	88	-16	29	10	155	74	297	13	Strike-slip
16	16	6	2010	0	52	57	-1.41	119.42	5.4	MW	12	348	66	0	79	90	-155	211	16	79	66	306	17	Strike-slip
17	12	5	2010	23	7	54	-1.28	120.11	5.1	MW	15.2	336	68	-16	73	75	-157	203	5	104	63	296	26	Strike-slip
18	8	1	2010	8	15	25	-0.5	120.00	4.8	MW	19.9	73	65	-179	343	89	-25	31	17	161	65	295	18	Strike-slip
19	2	3	2009	0	3	42	-1.05	119.99	5.6	MW	12.9	125	40	-93	309	50	-87	37	5	127	2	241	85	Normal
20	28	8	2007	8	51	41	-1.32	119.50	5.2	MW	16.1	28	19	95	202	71	88	109	64	203	2	294	26	Thrust
21	9	7	2005	23	59	16	-1.07	120.08	5.9	MW	12	80	44	-141	320	64	-53	24	11	121	33	278	55	Oblique-Normal
22	23	1	2005	21	2	34	-1.09	120.07	5.3	MW	20.9	68	54	-155	322	70	-39	18	10	119	47	279	42	Strike-slip
23	23	1	2005	20	10	19	-1.01	120.08	6.2	MW	12	90	41	-133	321	61	-59	29	11	125	27	279	61	Oblique-Normal
24	23	1	2005	19	59	46	-1.01	120.05	5.3	MW	12	76	52	-155	327	68	-42	25	10	124	43	285	45	Oblique-Normal
25	2	11	2004	21	48	17	-0.96	119.57	4.9	MW	26.5	351	63	-21	91	71	-151	219	5	121	56	313	33	Strike-slip
26	1	7	2002	8	11	7	-0.95	120.45	5.3	MW	15	271	34	-97	99	56	-86	186	11	277	4	25	78	Normal
27	14	2	2002	13	14	28	-1.31	120.09	5	MW	23	221	64	175	313	86	26	180	21	321	64	84	15	Strike-slip
28	28	12	2000	21	6	54	-0.62	120.25	5.4	MW	27.2	108	54	-150	359	66	-40	56	8	154	44	319	45	Strike-slip
29	3	1	1993	4	23	41	-1.17	120.08	5.7	MW	48.4	68	72	173	160	83	19	25	18	179	70	292	8	Strike-slip
30	2	3	1985	15	47	40	-1.32	119.38	6.6	MW	43.9	283	84	-3	14	87	-174	148	2	43	83	238	6	Strike-slip